

Synthesis, Structure and Molecular Modeling of a Zn^{II}-Phenolate Complex as a Model for Zn^{II}-Containing Tyrosinate Metalloenzymes

Mauricio Lanznaster,^{a,#} Ademir Neves,^{*,a} Ivo Vencato,^a Adailton J. Bortoluzzi,^a Hugo Gallardo,^a Sérgio P. Machado^b and Aline Moreno Chagas Assumpção^b

^aDepartamento de Química, Universidade Federal de Santa Catarina, 88040-900 Florianópolis – SC, Brazil

^bInstituto de Química, Universidade Federal do Rio de Janeiro, 21945-970 Rio de Janeiro – RJ, Brazil

Apresentamos neste trabalho a síntese, estrutura cristalina e as propriedades espectrais de ¹H NMR do complexo mononuclear [Zn^{II}(L-Br)].2H₂O o qual contém em sua primeira esfera de coordenação, o ligante hexadentado H₂L-Br (H₂L-Br = *N,N'*-bis-(5-bromo-2-hidróxibenzil)-*N,N'*-bis-(piridin-2-ilmetil)-1,2-etanodiamina). Cálculos teóricos utilizando DFT mostram boa correlação entre os parâmetros calculados e aqueles obtidos através de cristalografia de raios X em monocristais e revelam que somente os grupos fenolatos do ligante H₂L-Br participam na formação do HOMO, enquanto somente os anéis piridínicos contribuem para a formação do LUMO.

We describe herein the synthesis, crystal structure and ¹H NMR properties of the mononuclear [Zn^{II}(L-Br)].2H₂O complex containing the hexadentate H₂L-Br ligand (H₂L-Br = *N,N'*-bis-(5-bromo-2-hydroxybenzyl)-*N,N'*-bis-(pyridin-2-ylmethyl)-ethane-1,2-diamine). DFT calculations demonstrate very good agreement between parameters calculated and those determined by X-ray crystallography, and reveal that only the phenolate groups of the H₂L-Br ligand participate in the formation of the HOMO, while only one of the pyridine rings contributes to the LUMO formation.

Keywords: Zn^{II}-phenolate complex, crystal structure, ¹H NMR, DFT calculation

Introduction

Many Zn^{II}-containing enzymes have been discovered and their role in biological processes studied. Carbonic anhydrase,^{1,2} carboxypeptidase,³⁻⁵ β-lactamase II,⁶ thermolysin,⁷ alkaline phosphatase,⁸ and astacin^{9,10} are examples of such metalloenzymes. Of these, astacin, a digestive zinc-endopeptidase that is involved in hydrolytic processes should be highlighted since it represents the first example of a zinc enzyme that contains a tyrosine residue coordinated directly to the metal center in the active site.¹¹ In fact, astacin, an endopeptidase isolated from crawfish *Astacus astacus* represents the prototype for the “astacin family”,^{12,13} which includes mammalian metallo-endopeptidases¹⁴ and developmentally regulated human,¹⁵ fruitfly,¹⁶ frog¹⁷ and sea urchin¹⁸ proteins. The X-ray crystal structure of astacin (R-value of 0.162) reveals that the Zn^{II}-ion lies in a trigonal bipyramidal coordination environment

with three histidines, a water molecule and a more remote tyrosine as ligands.¹¹ One histidine nitrogen and the tyrosine OH group, at distances of 2.3 and 2.6 Å to the zinc, respectively, are apically connected, whereas the other three ligands are coplanar and 2.1 Å apart from the zinc center. Following our interest in the search for new compounds as structural and functional models for the active site of zinc-containing metalloenzymes,¹⁹⁻²¹ we report here the synthesis, X-ray structure and molecular modeling using Density Functional Theory (DFT) for the [Zn(L-Br)] complex, where L-Br²⁻ is the deprotonated form of the *N,N'*-bis-(5-bromo-2-hydroxy-benzyl)-*N,N'*-bis-(pyridin-2-ylmethyl)-ethane-1,2-diamine ligand. Importantly, theoretical calculations have been recently introduced in our group as a strategy for planning the synthesis of new ligands and model complexes.²²

Experimental

Abbreviations

H₂L-Br = *N,N'*-bis-(5-bromo-2-hydroxybenzyl)-*N,N'*-bis-(pyridin-2-ylmethyl)-ethane-1,2-diamine; H₂L¹ = (*N,N'*-bis-

* e-mail: ademir@qmc.ufsc.br

#Present address: Instituto de Química, Universidade Federal Fluminense, Campus do Valonguinho, s/n, Centro, 24020-150 Niterói - RJ

(2-hydroxybenzyl)-*N,N'*-bis-(pyridin-2-ylmethyl)-ethane-1,2-diamine); $H_2L^2 = (N,N'$ -bis-(2-hydroxybenzyl)-*N,N'*-bis-(pyridin-2-ylmethyl)-propane-1,3-diamine); $H_2L^3 = N,N'$ -bis-(5-nitro-2-hydroxybenzyl)-*N,N'*-bis-(pyridin-2-ylmethyl)-propane-1,3-diamine; Hbpa = *N*-(2-hydroxybenzyl)-*N*-(pyridin-2-ylmethyl)amine; DFT = Density Functional Theory.

Material and methods

All reagents and solvents were purchased from commercial sources and used as received. 1H NMR spectra were recorded on a Bruker 200 FT spectrometer, in $CDCl_3$ as a solvent. Infrared spectra were recorded with a Perkin Elmer FTIR 2000, in KBr pellets. Elemental analyses were performed with a Carlo Erba instrument model E-1110.

Synthesis of H_2L -Br

The H_2L -Br ligand was prepared according to the sequence of reactions depicted in Scheme 1, with slight modifications of the method described for the synthesis of the H_2bbpen ligand.²³ Ethylenediamine (10.0 mmol) was added dropwise to a THF/methanol - 2:1 solution of 2-hydroxy-5-bromobenzaldehyde (20.0 mmol) while stirring. After 30 min $NaBH_4$ (26.0 mmol) was added, and a few minutes later the deep yellow solution became colorless. Then, 4.0 mol L^{-1} HCl was added to adjust the pH to 7 and the solvent was removed under vacuum at 40 °C. Water was added to the precipitated product which was filtered off and washed with water followed by cold methanol. The white solid obtained (7.5 mmol) was added to a solvent mixture of THF and water 1:1 (100 mL) with 2-chloromethylpyridine hydrochloride (23 mmol) and sodium carbonate (38 mmol). This mixture was refluxed for 18 hours and the THF removed under vacuum at 40 °C. The residual water was decanted off and the product

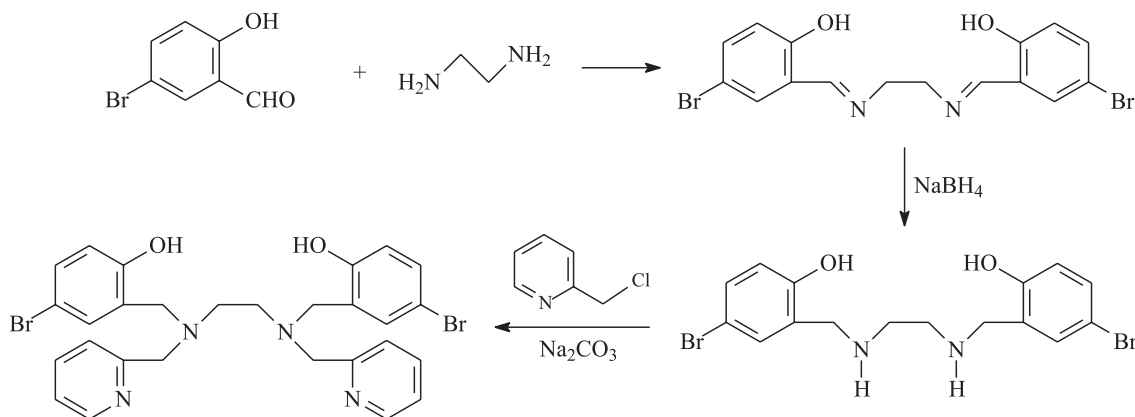
(yellowish oil) was solubilized in a mixture of 2-propanol and ethyl acetate. The H_2L -Br ligand precipitated as a white powder after 24 hours (yield = 75%). Anal. Calc. for H_2L -Br ($Br_2C_{28}H_{28}N_4O_2$): C, 54.92; H, 4.61; N, 9.15%. Found: C, 54.86; H, 4.73; N, 8.99%. IR (KBr pellet) ν_{max}/cm^{-1} : 1593(m), 1569(m), 1480(s), 1456(m), 1431(m), $\nu(C=C, C=N)$; 1271(s), 1236(m), $\nu(C-O)$.

Synthesis of $[Zn(L-Br)].2H_2O$

The $[Zn(L-Br)].2H_2O$ complex was prepared by the reaction of $Zn(OAc)_2.2H_2O$ (1 mmol) with H_2L -Br (1 mmol) in methanol while stirring at 45 °C for 30 min. After evaporation of the solvent, the crude oil was dissolved in chloroform and washed with a $NaHCO_3$ (5% aqueous solution) in a separation funnel. The organic layers were combined, dried with anhydrous Na_2SO_4 and concentrated at reduced pressure. The resulting colourless oil was crystallized from an ethylacetate/methanol (1:1) solution (yield = 70%), providing suitable crystals for X-ray crystallography analysis. Anal. Calc. for $[Zn(L-Br)].2H_2O$ ($C_{28}H_{32}N_4O_4Br_2Zn$): C, 47.12; H, 4.52; N, 7.85%. Found: C, 47.35; H, 4.97; N, 7.79%. IR (KBr pellet) ν_{max}/cm^{-1} : 1606(w), 1585(w), 1471(s), 1440(w), 1413(w), $\nu(C=C, C=N)$; 1274(s), $\nu(C-O)$.

Crystal structure determination

A colorless irregular block was prepared from a big crystal, which was selected from the crystalline sample of the $[Zn(L-Br)]$ complex. The crystal data were measured on an Enraf-Nonius CAD4 diffractometer, using graphite monochromated Mo- K_α radiation ($\lambda=0.71069$ Å), at room temperature. Cell parameters were determined from 25 carefully centered reflections in the q range 8.76–15.30° and refined by the least-squares method. The collected intensities were corrected for Lorentz and polarization effects²⁴ and for



Scheme 1.

absorption (face-indexed method; T_{\min} 0.28 and T_{\max} 0.64). The structure was solved by direct methods and was refined by the full-matrix least-squares method using SHELXS97²⁵ and SHELXL97²⁶ computer programs, respectively. All non-hydrogen atoms were refined with anisotropic displacement parameters. H atoms bonded to C atoms were placed at idealized positions using standard geometric criteria, whereas the H atoms of the water molecule of crystallization were found from Fourier map and treated with a riding model. Further relevant crystallographic data are summarized in Table 1. The drawing of molecular structure was made with ORTEP3 program.²⁷

Computational details

All geometry optimizations were performed with B3LYP hybrid density functional theory in conjunction with the 6-31G (d,p) basis set and LACVP* basis set for the metal using the Spartan 04 program.²⁸ The calculations were carried out on a 2.6 GHz Athlon PC, with 1 GB RAM and 40Gb HD under the operational system Windows 2000, using the Spartan 04 program.

Results and Discussion

Syntheses

The H₂L-Br ligand was obtained in a good yield and pure enough to be fully characterized and used as a precursor for the synthesis of coordination compounds. The reaction between one equivalent of H₂L-Br and one equivalent of Zn(OAc)₂·2H₂O produced the mononuclear complex [Zn(L-Br)]·2H₂O. Infrared spectral data reveal that upon coordination of H₂L-Br to the zinc there is a general bathochromic shift of ~15 cm⁻¹ and a decrease in intensity of the C=N and C=C stretching modes. Interestingly, dinuclear [ZnL].ZnCl₂ complexes were reported by Adams *et al.*²⁹ for the reaction between the similar ligands H₂L¹ (H₂L¹ = *N,N'*-bis-(2-hydroxybenzyl)-*N,N'*-bis-(pyridin-2-ylmethyl)-ethane-1,2-diamine) and H₂L² (H₂L² = *N,N'*-bis-(2-hydroxybenzyl)-*N,N'*-bis-(pyridin-2-ylmethyl)-propane-1,3-diamine)³⁰ with ZnCl₂, in a 1:1 stoichiometry. In these homodinuclear compounds, the coordinated phenolate oxygen atoms act as ligands toward a second zinc-containing entity yielding [ZnL].ZnCl₂. The reaction between H₂L² and Zn(OAc)₂ also produced a dinuclear species [Zn(L²)-Zn(OAc)₂], according to Adams's report. A mononuclear [ZnL³] species was only obtained with the ligand H₂L³ (H₂L³ = *N,N'*-bis-(5-nitro-2-hydroxybenzyl)-*N,N'*-bis-(pyridin-2-ylmethyl)-propane-1,3-diamine), due the electron

withdrawing effect of the nitro group which makes the phenolic oxygen atoms weaker Lewis bases and consequently less able to coordinate a second zinc atom.^{29,30} The fact that the mononuclear species [Zn(L-Br)] described herein was obtained, instead of a dinuclear molecule, indicates that the electron withdrawing effect of the bromo groups in H₂L-Br is working in the same way as the nitro groups in Fenton's H₂L³, which suggests that the ligand substituent groups are playing an important role in the reaction stoichiometry.

Crystal structure of [Zn(L-Br)]·2H₂O

The molecular structure of the [Zn(L-Br)] molecule in [Zn(L-Br)]·2H₂O is depicted in Figure 1. Crystallographic data are shown in Table 1, and selected bond lengths and angles are listed in Table 2. The complex [Zn(L-Br)] consists of a distorted octahedral molecule, with the hexadentate N₄O₂-donor ligand binding the Zn^{II}-ion *via* two amine nitrogen atoms of the ethylenediamine backbone, two phenol oxygen atoms and two pyridine nitrogen atoms. Each half of the ligand provides a facial N₂O-donor set with the phenolate oxygen atoms *cis* to each other and *trans* to the aliphatic nitrogen atoms. Completing the coordination sphere, the pyridine nitrogen atoms occupy apical sites and are *trans* to each other. This structural arrangement is essentially similar to that reported for [ZnL³],³⁰ except for the fact that [Zn(L-Br)] contains an ethylenediamine backbone instead of a propane-1,3-diamine backbone in [ZnL³]. Consequently, the [Zn(L-Br)] complex presents a higher distorted geometry due to its five-membered ring in the equatorial plane compared to the six-membered ring in [ZnL³]. The higher distortion in [Zn(L-Br)] can be evidenced by the three *trans* angles which are 3.5° (N1-Zn-O2), 4.8° (N2-Zn-O1) and 11.1° (N31-Zn-N41) smaller for [Zn(L-Br)] when compared to [ZnL³]. The average Zn-O bond lengths for [Zn(L-Br)] (1.997 Å) are 0.063 Å shorter than those for [ZnL³]. This is attributed to the higher distortion in the coordination sphere and the weaker electron-withdrawing effect of the bromo groups in [Zn(L-Br)]. On the other hand, the average Zn-N_{py} bond lengths are 0.058 Å longer in [Zn(L-Br)] when compared to [ZnL³], whereas the Zn-N_{amine} bonds are identical in both complexes.

Since the [Zn(L-Br)] and the [Zn(bpa)₂]¹⁹ complexes (Hbpa = *N*-(2-hydroxybenzyl)-*N*-(pyridin-2-ylmethyl)amine) possess identical coordination environments, a comparison of their structural parameters should also be of interest. Firstly, it should be noted that H₂L-Br is a hexadentate N₄O₂ ligand bound to the Zn^{II}-ion in its

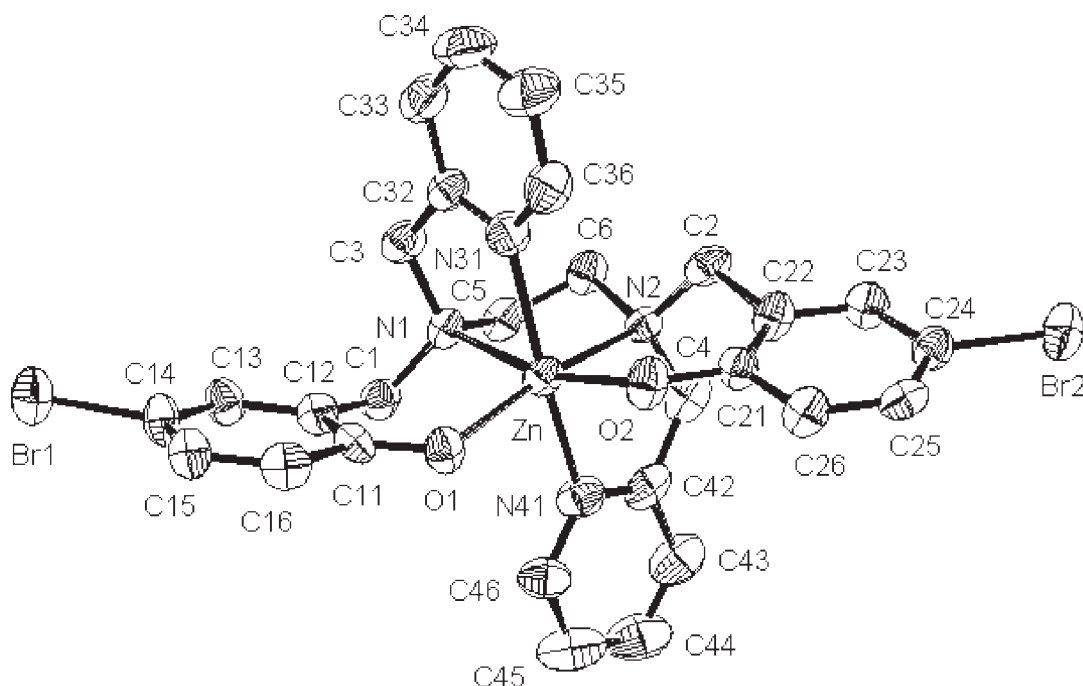


Figure 1. ORTEP of [Zn(L-Br)] with atom-labeling scheme and ellipsoids at 40% probability.

Table 1. Crystal data and structure refinement for [Zn(L-Br)].2H₂O

Formula	C ₂₈ H ₂₈ Br ₂ N ₄ O ₃ Zn
Formula weight	693.73
T	293(2) K
λ	0.71073 Å
Crystal system	Monoclinic
Space group	P2 ₁ /n
Cell parameters	a = 12.783(1) Å b = 16.242(2) Å c = 13.916(2) Å β = 100.65(1)°
V	2839.5(6) Å ³
Z	4
ρ Density (calculated)	1.623 g cm ⁻³
μ	3.716 mm ⁻¹
F(000)	1392
Crystal size	0.46 x 0.26 x 0.13 mm
Theta range for data collection	1.95 to 25.00°
Index ranges	-15 ≤ h ≤ 14; 0 ≤ k ≤ 19; 0 ≤ l ≤ 16
Reflections collected	5203
Independent reflections	4986 (R(int) = 0.0860)
Refinement method	Full-matrix least-squares on F ²
Data / restraints / parameters	4986 / 0 / 343
Goodness-of-fit on F ²	0.963
Final R indices [I > 2σ(I)]	R ₁ = 0.0626, wR ₂ = 0.1351
R indices (all data)	R ₁ = 0.2101, wR ₂ = 0.1732
Largest diff. peak and hole	0.778 and -0.779 e.Å ⁻³

Table 2. Selected calculated and experimental bond lengths (Å) and angles (°) for [Zn(L-Br)]

	Experimental	Calculated
Zn-O1	1.983(6)	1.997
Zn-O2	2.011(6)	2.016
Zn-N1	2.249(7)	2.393
Zn-N2	2.270(7)	2.412
Zn-N31	2.206(8)	2.272
Zn-N41	2.202(8)	2.268
C5-C6	1.508(12)	1.534
O1-Zn-O2	100.4(2)	111.51
O2-Zn-N2	89.4(2)	88.08
O2-Zn-N1	163.9(3)	155.33
O2-Zn-N41	97.3(3)	91.98
O2-Zn-N31	90.2(3)	87.61
O1-Zn-N2	163.1(3)	154.43
O1-Zn-N1	90.9(2)	88.69
O1-Zn-N41	89.0(3)	89.29
O1-Zn-N31	100.7(3)	103.21
N1-Zn-N2	82.5(2)	77.54
N41-Zn-N2	76.1(3)	73.19
N31-Zn-N2	92.8(3)	93.54
N41-Zn-N1	94.2(3)	102.66
N31-Zn-N1	76.5(3)	73.59
N41-Zn-N31	166.5(3)	166.72

deprotonated form, while in [Zn(bpa)₂] the Hbpa ligand corresponds to the half of H₂L-Br without the ethylenediamine backbone and the bromo substitution in the *para*-position of the phenolate group (tridentate N₂O-donor). Consequently, in [Zn(L-Br)] the tertiary amine nitrogen atoms must be coordinated in a *cis*-position

to each other excluding the possibility of an inversion center at the zinc. Secondly, in both complexes the *N*-(2-hydroxybenzyl)-*N*-(pyridin-2-ylmethyl)amine unity adopts a facial coordination arrangement. However, in [Zn(bpa)₂] the atoms of the same nature (two N_{amine}, two N_{pyridine} and two O_{phenolate}) are coordinated in *trans* positions

with respect to each other since the molecule has an inversion center. Thus, the Zn-O distances in [Zn(bpa)₂] are ~ 0.1 Å longer than those detected in [Zn(L-Br)], while the Zn-N_{amine} distances are 0.1 Å shorter. This fact is most probably a reflection of distinct *trans*-influence of the phenolate groups in these complexes. As expected, the Zn-N_{pyridine} bond distances (av. 2.16 Å in [Zn(bpa)₂] and av. 2.26 Å in [Zn(L-Br)]) are comparable and fall into the range of Zn-N_{pyridine} distances observed for other octahedral Zn^{II} complexes already reported in the literature.^{19,20,29,30} Finally, this structural arrangement of H₂L-Br around the zinc in [Zn(L-Br)] has also been observed in M^{III} complexes (M^{III} = V, Mn, Fe, Ga, In) with H₂L¹ and its chloro and bromo derivatives.^{23,31-33} An exception is the [Ru(bbpen)]⁺ cation complex which shows two amine nitrogens, two pyridine nitrogens and two phenolate oxygen atoms all as *cis* pairs.³⁴

The coordination of phenolate moieties in *cis* positions to the metal center induces a intermolecular bifurcated H bond formation, where the water molecule of crystallization is the donor group (O1W-H1WA 0.88 Å) and the oxygen atoms O1 (H1WA...O1 2.29 Å; O1W...O1 3.00(1) Å; <O1W-H1WA...O1 138.7 °) and O2 (H1WA...O2 2.16 Å; O1W...O2 2.84(1) Å; <O1W-H1WA...O2 133.7 °) are the acceptors. The bromine atoms are also involved in observed

short contacts with neighboring H atoms (H46...Br2 3.01 Å, <C46-H46...Br2 143.0°; H15...Br2 3.04 Å, C15-H15...Br2 130.1°).

¹H NMR spectrum of [Zn(L-Br)]·2H₂O

Since the [Zn(L-Br)] complex is diamagnetic, ¹H NMR was used to investigate the species in CDCl₃ solution. The room-temperature ¹H NMR spectra, 200 MHz (Figure 2) clearly indicate the formation of the complex, and confirm that the symmetric solid-state structure is retained in solution. The assignments of all protons in the ligand and in the corresponding complex are based on the intensity of the signals and spin-spin splitting structure. The ¹H NMR spectra for the free ligand and the corresponding [Zn(L-Br)] complex, depicted in Figure 2, contain seven unique protons resonances in the aromatic region with some small differences, indicating that complexation has taken place. The pyridine H⁶ hydrogen atoms are shifted downfield by 0.37 ppm for [Zn(L-Br)], relative to their positions in the free ligand spectrum. A 0.33 ppm upfield shift is also observed for the phenyl H⁶ hydrogen atoms in the [Zn(L-Br)] spectrum. The most remarkable differences between the ligand and the complex are the resonances in the aliphatic region for the methylene groups. The free ligand,

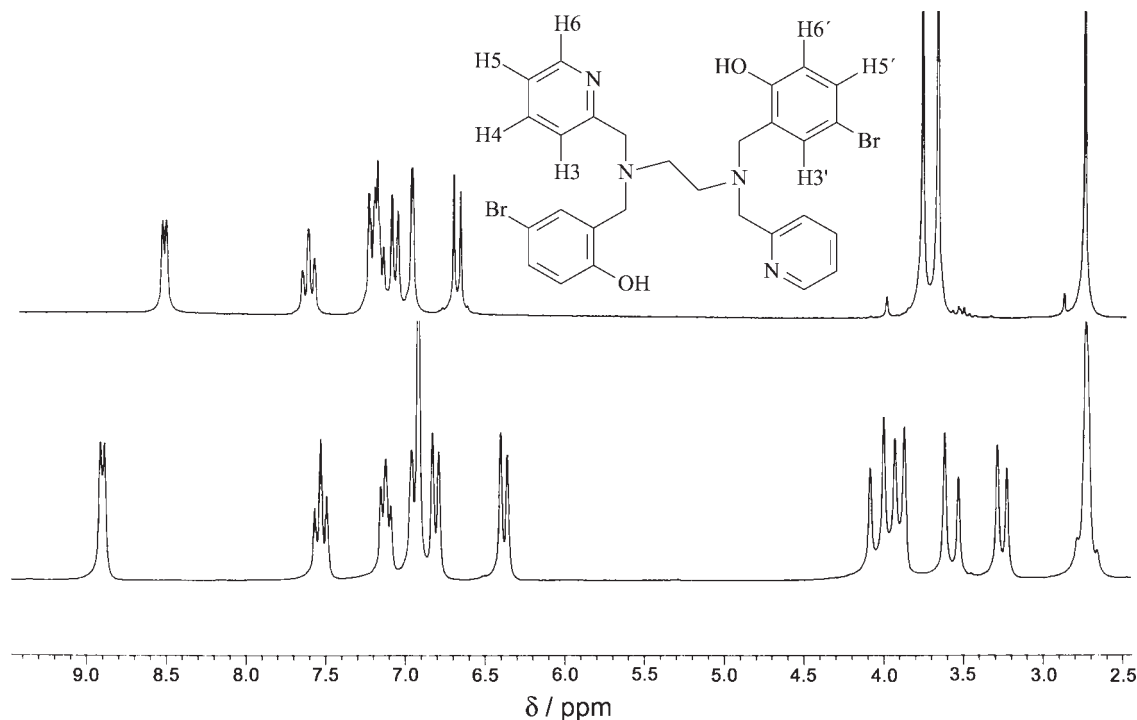


Figure 2. ¹H NMR spectra (200 MHz) in CDCl₃ of H₂L-Br (top) and [Zn(L-Br)] (bottom). [H₂L-Br]: δ 8.56 (d, 2H⁶, *J* 4.8 Hz, py); 7.64 (dt, *J* 7.6 Hz, 2H⁴, py); 7.26-7.17 (m, 4H, 2H⁵, 2H^{5'}); 7.09 (d, *J* 7.6 Hz, 2H³, py); 6.98 (d, *J* 1.9 Hz, 2H^{3'}, ph); 6.69 (d, *J* 8.7 Hz, 2H⁶, ph); 3.72 (s, 4H, -CH₂-py); 3.63 (s, 4H, -CH₂-ph); 2.68 (s, 4H, NCH₂CH₂N). [Zn(L-Br)]: δ 8.93 (d, 2H⁶, *J* 4.9 Hz, py); 7.55 (dt, 2H⁴, *J* 7.6 Hz, py); 7.16 (t, 2H⁵, *J* 6.3 Hz, py); 6.96-6.91 (m, 2H^{3'}, 2H^{5'}, ph); 6.83 (d, 2H³, *J* 7.8 Hz, py); 6.36 (d, 2H⁶, *J* 8.3 Hz, ph); 4.08 (d, 2H_a, *J* 17.0 Hz, -CH_aH_b-py); 3.93 (d, 2H_a, *J* 11.7 Hz, -CH_aH_b-ph); 3.60 (d, 2H_b, *J* 17.0 Hz, -CH_aH_b-py); 3.26 (d, 2H_b, *J* 11.7 Hz, -CH_aH_b-ph); 2.68 (s, 4H, NCH₂CH₂N).

H_2L-Br , contains three prochiral CH_2 groups with enantiotopic Hs isolated from the others. The Hs are observed as three singlet peaks shifted upfield to 3.72 (s, 4H, $-CH_2-py$), 3.63 (s, 4H, $-CH_2-ph$) and 2.68 ppm (s, 4H, $-NCH_2CH_2N-$). The $[Zn(L-Br)]$ complex also contains three prochiral CH_2 groups, two groups with diastereotopic Hs ($-CH_aH_b-py$; $-CH_aH_b-ph$), and one with enantiotopic Hs ($-NCH_2CH_2N-$), all isolated from the other Hs. These Hs are observed as two pairs of doublets in the case of the diastereotopic Hs, with high geminal coupling constants at 4.08 (d, $2H_a$, J 17 Hz, $-CH_aH_b-py$), 3.93 (d, $2H_a$, J 11.7 Hz, $-CH_aH_b-ph$), 3.60 (d, $2H_b$, J 17.0 Hz, $-CH_aH_b-py$), and 3.26 ppm (d, $2H_b$, J 11.7 Hz, $-CH_aH_b-ph$) and a singlet in the case of the enantiotopic Hs at 2.68 ppm (s, 4H, $-NCH_2CH_2N-$).

Theoretical calculations

The results for the principal calculated and experimental (for comparison) structural parameters of the $[Zn(L-Br)]$ complex are shown in Table 2 and the optimized structure is shown in Figure S1 in the Supplementary Information. The maximum variation for the bond lengths is 0.16 Å and for angles is 9.1° . A comparison between the geometric parameters of the model and the experimental data shows that the results are in good agreement. The difference noted is due to the fact that the model complexes were considered in the gas phase while the experimental parameters were measured in crystalline form. The graphical representation

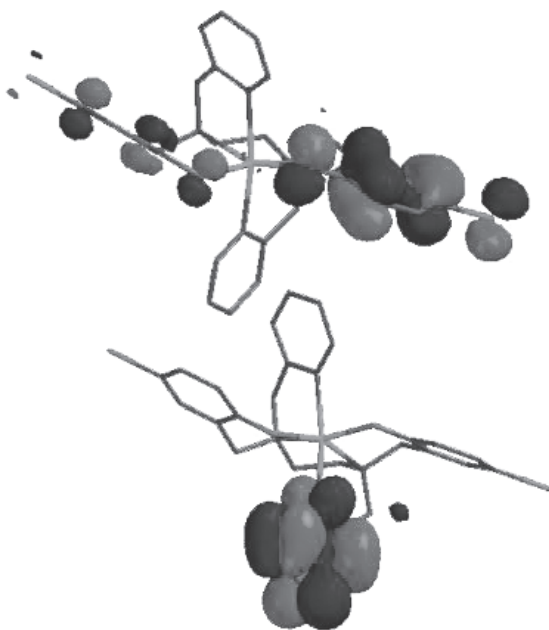


Figure 3. Graphical representation of HOMO (top) and LUMO (bottom) for $[Zn(L-Br)]$.

of HOMO shows that only the phenolate rings participate in its formation (Figure 3 top). On the other hand, only one of the pyridinic rings contributes to the LUMO formation (Figure 3 bottom). The surface of electrostatic potential shows once again that the electronic density of the complex is localized around the phenolic rings. It can also be noted that the bromide substitutions pull the electronic density to the halogen atom (Figure S2 in the Supplementary Information).

Conclusions

Only recently mononuclear Zn^{II} -phenolate containing complexes have been reported.^{19,20,29,30} In this paper we described the synthesis, crystal structure and 1H NMR properties of such a complex. The good agreement between the theoretical and experimental data obtained for $[Zn(L-Br)]$ indicates that the use of DFT is appropriate in the planning and synthesis of new structural and functional models for Zn^{II} -containing phenolate enzymes. Based on this information, the synthesis of further multidentate ligands containing phenol as a coordinating group are under investigation, and will be the subject of further reports.

Supplementary Information

The crystallographic data (atomic coordinates and equivalent isotropic displacement parameters, calculated hydrogen atom parameters, anisotropic thermal parameters and bond lengths and angles) have been deposited at the Cambridge Crystallographic Data Center (deposition number CCDC 261524). Copies of this information may be obtained free of charge from: CCDC, 12 Union Road, Cambridge, CB2 1EZ, UK (Fax: +44-1223-336-033; e-mail: deposit@ccdc.cam.ac.uk or <http://www.ccdc.cam.ac.uk>). Figures S1 and S2 showing the optimized structure and the electrostatic potential surface for $[Zn(L-Br)]$, respectively are available free of charge via internet at <http://jbc.sbj.org.br>

Acknowledgments

This work was supported by grants from CNPq, FINEP, FAPERJ and Fundação José Pelúcio Ferreira.

References

1. Kannan, K.K.; Notstrand, B.; Fridborg, K.; Lovgren, S.; Ohlsson, A.; Petef, M.; *Proc. Nat. Acad. Sci. U.S.A.* **1975**, *72*, 51.
2. Liljas, A.; Kannan, K.K.; Bergsten, P.C.; Waara, I.; Fridborg, K.; Strandberg, B.; Carlbom, U.; Jarup, L.; Lovgren, S.; Petef, M.; *Nature* **1972**, *235*, 131.

3. Dideberg, O.; Charlier, P.; Dive, G.; Joris, B.; Frere, J.M. Ghuysen; J.M.; *Nature* **1982**, 299, 469.
4. Quijoch, F.A.; Lipscomb, W.N.; *Adv. Protein Chem.* **1971**, 25, 1.
5. Schmid, M.F.; Herriott, J.R.; *J. Mol. Biol.* **1976**, 103, 175.
6. Sutton, B. J.; Artymiuk, P.J.; Cordero-Borboa, A.E.; Little, C.; Phillips, D.C.; Waley, S.G.; *Biochem. J.* **1987**, 248, 181.
7. Matthews, B.W.; Jansonius, J.N.; Colman, P.M.; Schoenborn, B.P.; Dupourque, D.; *Nature, New Biol.* **1972**, 238, 37.
8. Kim, E.E.; Wyckoff, H.W.; *J. Mol. Biol.* **1991**, 218, 449.
9. Stocker, W.; Wolz, R.L.; Zwilling, R.; Strydom, D.J.; Auld, D.S.; *Biochemistry* **1988**, 27, 5026.
10. Titani, K.; Torff, H. J.; Hormel, S.; Kumar, S.; Walsh, K.A.; Rodl, J.; Neurath, V.; Zwilling, R.; *Biochemistry* **1987**, 26, 222.
11. Bode, W.; Gomis-Ruth, F.X.; Huber, R.; Zwilling, R.; Stocker, W.; *Nature* **1992**, 358, 164.
12. Stocker, W.; Sauer, B.; Zwilling, R.; *Biol. Chem. Hopper-Seyler* **1991**, 372, 385.
13. Barrett, A.J.; Rawlings, N.D.; *Biochem. Soc. Trans.* **1991**, 19, 707.
14. Dumermuth, E.; Sterchi, E.E.; Jiang, W.P.; Wolz, R.L.; Bond, J.S.; Flannery, A.V.; Beynon, R.J.; *J. Biol. Chem.* **1991**, 266, 21381.
15. Wozney, J.M.; Rosen, V.; Celeste, A.J.; Mitscock, L.M.; Whitters, M.J.; Kriz, R.W.; Hewick, R.M.; Wang, E.A.; *Science* **1988**, 242, 1528.
16. Shimell, M.J.; Ferguson, E.L.; Childs, S.R.; O'Connor, M.B.; *Cell* **1991**, 67, 469.
17. Sato, S.M.; Sargent, T.D.; *Dev. Biol.* **1990**, 137, 135.
18. Reynolds, S.D.; Angerer, L.M.; Palis, J.; Nasir, A.; Angerer, R.C.; *Development* **1992**, 114, 769.
19. Neves, A.; Vencato, I.; Verani, C.N.; *J. Braz. Chem. Soc.* **1997**, 8, 265.
20. Correia, V.R.; Bortoluzzi, A.J.; Neves, A.; Joussef, A.C.; Vieira, M.G.M.; Batista, S.C.; *Acta Cryst. E* **2003**, 59, m464.
21. Lanznaster, M.; Neves, A.; Bortoluzzi, A. J.; Szpoganicz, B.; Schwingel, E.; *Inorg. Chem.* **2002**, 41, 5641.
22. Paes, L.W.; Faria, R.B.; Machuca-Herrera, J.O.; Neves, A.; Machado, S.P.; *Can. J. Chem.* **2004**, 82, 1619.
23. Neves, A.; Ceccato, A.S.; Erthal, S.M.D.; Vencato, I.; *Inorg. Chim. Acta* **1991**, 187, 119.
24. Spek, A. L.; *HELENA: CAD-4 Data Reduction Program*; Univ. of Utrecht, The Netherlands, 1996.
25. Sheldrick, G.M.; *SHELXS97: Program for the Solution of Crystal Structures*. University of Göttingen, Germany, 1990.
26. Sheldrick, G.M.; *SHELXL97: Program for the Refinement of Crystal Structures*. University of Göttingen, Germany, 1997.
27. Farrugia, L. J.; *J. Appl. Crystallogr.* **1997**, 30, 565.
28. Spartan 04, *Wavefunction Inc.*, Irvine, CA, 92612 USA, 2004.
29. Adams, H.; Bradshaw, D.; Fenton, D.E.; *Eur. J. Inorg. Chem.* **2001**, 859.
30. Adams, H.; Bradshaw, D.; Collison, D.; Fenton, D.E.; *Inorg. Chem. Commun.* **2001**, 4, 664.
31. Neves, A.; Erthal, S.M.D.; Vencato, I.; Ceccato, A.S.; Mascarenhas, I.; Nascimento, O.R.; Horner, M.; Batista, A.A.; *Inorg. Chem.* **1992**, 31, 4749.
32. Setyawati, I. A.; Rettig, S.J.; Orvig, C.; *Can. J. Chem.* **1999**, 77, 2033.
33. Wong, E.; Liu, S.; Rettig, S.J.; Orvig, C.; *Inorg. Chem.* **1995**, 34, 3057.
34. Neves, A.; Brito, M.A.; Oliva, G.; Nascimento, O.R.; Panepucci, E.H.; Souza, D.H.F.; Batista, A.A.; *Polyhedron* **1995**, 14, 1307.

Received: September 22, 2005

Published on the web: February 13, 2006

Synthesis, Structure and Molecular Modeling of a Zn^{II}-Phenolate Complex as a Model for Zn^{II}-Containing Tyrosinate Metalloenzymes

Mauricio Lanznaster,^{a,§} Ademir Neves,^{*,a} Ivo Vencato,^a Adailton J. Bortoluzzi,^a Hugo Gallardo,^a
Sérgio P. Machado,^b and Aline Moreno Chagas Assumpção^b

^aDepartamento de Química, Universidade Federal de Santa Catarina, 88040-900 Florianópolis – SC, Brazil

^bInstituto de Química, Universidade Federal do Rio de Janeiro, 21945-970 Rio de Janeiro – RJ, Brazil

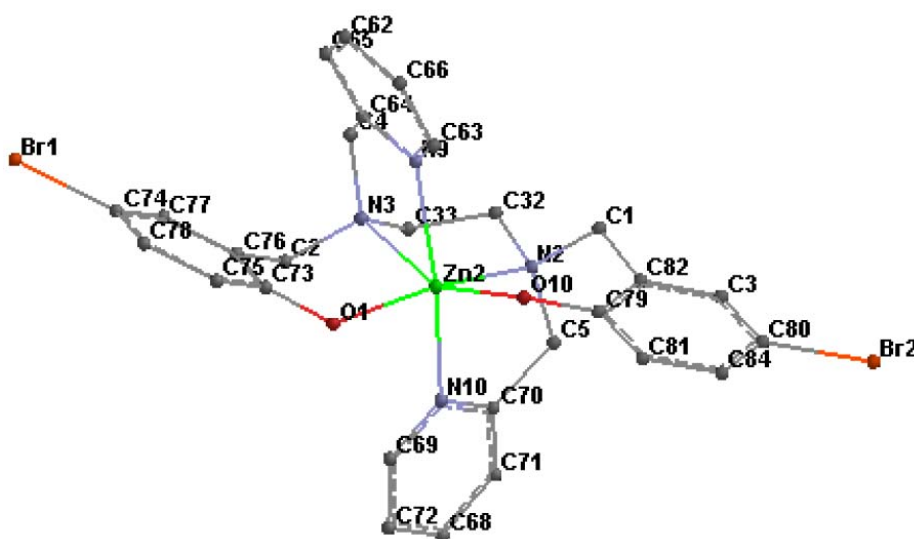


Figure S1. Optimized structure of the [Zn(L-Br)].

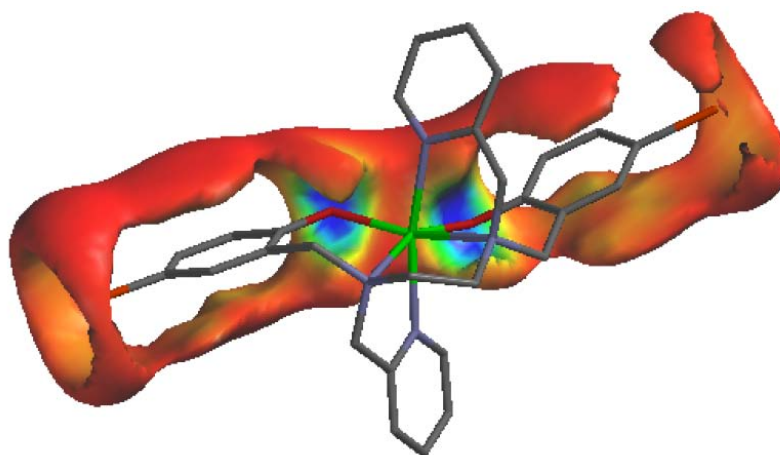


Figure S2. Electrostatic potential surface for [Zn(L-Br)].

* e-mail: ademir@qmc.ufsc.br